J. Physiol. (1973), **235**, *pp.* 103–131
With 12 text-figures
Printed in Great Britain

RECONSTRUCTION OF THE ACTION POTENTIAL OF FROG SARTORIUS MUSCLE

BY R. H. ADRIAN AND L. D. PEACHEY

From the Physiological Laboratory, University of Cambridge, Cambridge
and the Department of Biology, University of Pennsylvania, Pa., U.S.A.

(*Received 26 April 1973*)

SUMMARY

1. Propagated action potentials of striated muscle are calculated using an equivalent circuit that represents the transverse tubular system as a radial cable of sixteen elements. The membrane of the transverse tubules is assumed to have activatable ionic currents similar to those in the fibre surface.

2. The configuration of the after-potential and the conduction velocity are best accounted for by postulating a resistance of about 150 Ω cm^2 separating the extracellular fluid from the lumen of the transverse tubules at the edge of the fibre, and a density of sodium channels in the tubular wall about a twentieth of that in the fibre surface.

3. Calculations with imposed voltage steps at the fibre surface suggest that the potential across the tubular membrane at the centre of the fibre is very far from clamped.

4. Currents providing charge for the tubular capacity can give rise to substantial errors in estimating the zero-current potential of the ionic currents.

INTRODUCTION

In a previous paper (Adrian, Chandler & Hodgkin, 1970) the action potential of frog striated muscle was reconstructed from voltage-clamp results. The reconstructions were based on the equivalent circuit of the membrane suggested by Falk & Fatt (1964) in which the transverse tubular system is represented by a linear resistance and capacity in series (R_s and C_T in Adrian *et al.* 1970). There were several deficiencies in the reconstructed action potential and it was pointed out that these might arise if sodium current, or some other type of active current were present in the tubular system. Costantin's (1970) observations have made the existence of a tubular sodium current very likely, and it seemed worth while to extend the

analysis of the action potential. Using a distributed parameter model for the tubular system, and taking account of tubular ionic currents carried by sodium and potassium, we have been able to give a more plausible description of the after potential and to show how Adrian *et al.* (1970) may have inaccurately estimated the zero-current potentials of the sodium channel (V'_{Na}) and of the delayed rectifier (V'_K). Peachey (1973) has given a short account of some of these findings.

THEORY

For an action potential propagating at a velocity θ, the cable equation can be written (Hodgkin & Huxley, 1952)

$$\frac{d^2V}{dt^2} = \frac{2\theta^2 R_i}{a} I_m, \tag{1}$$

where V is the potential across the fibre surface and is the potential that experimentally can be recorded; I_m is the current (A cm^{-2}) flowing between the sarcoplasm and the extracellular fluid; R_i is the resistivity of the sarcoplasm (Ω cm); a is the fibre radius.

$$I_m = I_i + I_T + C_m \frac{dV}{dt}, \tag{2}$$

where I_i is the ionic current (A cm^{-2}) through a square centimetre of the surface membrane; C_m is the capacity (μF cm^{-2}) of the surface membrane; and I_T the current (A cm^{-2}) entering or leaving the transverse tubular system connected to a square centimetre of fibre surface. I_T is composed of ionic and capacity current flowing across the tubular walls. Combining (1) and (2),

$$\frac{d^2V}{dt^2} = K\left(\frac{I_i + I_T}{C_m} + \frac{dV}{dt}\right), \tag{3}$$

where

$$K = 2\theta^2 R_i C_m / a.$$

If the transverse tubular system can be considered as a network of capacities and linear conductances, the potential (u) across the wall of the tubules will be described by eqn. (4), which is equivalent to the equation given by Adrian, Chandler & Hodgkin (1969)

$$\frac{1}{r}\frac{\partial}{\partial r}\left(r\frac{\partial u}{\partial r}\right) = \nu^2 u + \frac{1}{\kappa}\frac{\partial u}{\partial t}, \tag{4}$$

where

$$\nu^2 = \frac{1}{\lambda_T^2} = \frac{\bar{G}_W}{\bar{G}_L}, \quad \kappa = \frac{\bar{G}_L}{\bar{C}_W}. \tag{5}$$

$\bar{G}_L$, $\bar{G}_W$ and $\bar{C}_W$ are related to the tubular lumen conductivity (G_L) and the conductance (G_W) and capacity (C_W) of 1 cm^2 of tubular membrane by the following equations

$$\bar{G}_L = G_L \rho \sigma, \tag{6}$$

$$\bar{G}_W = G_W \rho / \zeta, \tag{7}$$

$$\bar{C}_W = C_W \rho / \zeta, \tag{8}$$

where ρ is the fraction of the muscle volume occupied by tubules ($\rho = 0{\cdot}003$); ζ is the volume to surface ratio of the tubules ($\zeta = 10^{-6}$ cm); and σ is a network geometric factor ($\sigma = 0{\cdot}5$). The values of ρ and ζ are taken from Peachey (1965). For the origin of σ see Adrian *et al.* (1969).

We assume that there is a resistance (R_s, Ω cm^2) the access resistance, which separates the lumen of the transverse tubules from the extracellular fluid (Peachey & Adrian, 1973). Physically this might correspond to the fact that the mouths of the tubules seem widely separated in the circumference of the fibre (Huxley & Taylor, 1958) or narrowing or tortuosity of the tubules near their mouths. Such an access resistance makes the boundary condition for eqn. (4) at $r = a$

$$V - u_a = R_s \bar{G}_L \left(\frac{\partial u}{\partial r}\right)_{r=a}, \tag{9}$$

where u_a is the potential across the wall of the transverse tubular system at the inner end of the access resistance. An alternative boundary condition that $u_a = V$, was used by Adrian *et al.* (1969). It is equivalent to the assumption that there is no access resistance.

If V rises exponentially as it does in the early stages of an action potential

$$V = V_R + \Delta V \exp(\mu t). \tag{10}$$

V_R is the resting potential across both the surface and tubular membranes. A similar exponentially rising potential will satisfy eqn. (4) and the boundary condition eqn. (9) if

$$u = V_R + \omega \exp(\mu t), \tag{11}$$

where $\omega = \Delta u = f(r)$ and is a solution of

$$\frac{1}{r}\frac{d}{dr}\left(r\frac{d\omega}{dr}\right) = \phi^2 \omega, \tag{12}$$

and $\phi^2 = \nu^2 + \mu/\kappa$. Since ω is bounded at $r = 0$ and $\omega = \Delta u_a$ at $r = a$

$$\omega = \frac{\Delta u_a I_0(r\phi)}{I_0(a\phi)} \tag{13}$$

and

$$u = V_R + \Delta u_a \frac{I_0(r\phi)}{I_0(a\phi)} \exp(\mu t). \tag{14}$$

$I_0(\ )$ are modified Bessel functions of zero order. The radial current at $r = a$ is equal to I_T

$$I_T = \bar{G}_L \left(\frac{\partial u}{\partial r}\right)_{r=a} = \bar{G}_L \Delta u_a \phi \frac{I_1(a\phi)}{I_0(a\phi)} \exp(\mu t). \tag{15}$$

Inserting (14) and (15) into (9)

$$\frac{\Delta u_a}{\Delta V} = \frac{I_0(a\phi)}{I_0(a\phi) + R_s \bar{G}_L \phi I_1(a\phi)}. \tag{16}$$

In the initial stages of the propagated action potential one can assume $I_1 = g_0(V - V_R)$ so that V, I_1 and I_T are all rising exponentially with a rate constant μ. Therefore, from eqn. (3)

$$\mu^2 = K\left[\frac{g_0}{C_M} + \frac{\bar{G}_L}{C_M}\frac{\Delta u_a \phi I_1(a\phi)}{\Delta V} \frac{}{I_0(a\phi)} + \mu\right], \tag{17}$$

which may be rewritten as

$$\mu^2 - K\mu - \frac{Kg_0}{C_m} = \frac{K\bar{G}_L \phi I_1(a\phi)}{C_m\{I_0(a\phi) + R_s \bar{G}_L \phi I_1(a\phi)\}}. \tag{18}$$

Provided the propagation constant K is known, or can be estimated, μ can be obtained from this transcendental equation which has one positive real root and infinitely many real negative roots. Eqns. (14) and (16) allow one to calculate u and du/dt throughout the tubular network for a small value of ΔV (0·1 mV). These values of ΔV, dV/dt and u constitute initial values for computing the propagated action potential.

In a calculation of the action potential and the potential changes in the tubular system from eqns. (3), (4) and (9) it would be necessary to integrate simultaneously with respect to r as well as t. To avoid integrating with respect to r, the transverse tubular system is divided into one central disk and fifteen concentric annuli. The radius of the central disk and the radial thickness of each annulus is $\frac{1}{16}a$. The conductances ($g_{T(1)}$ to $g_{T(16)}$) and capacities ($c_{T(1)}$ to $c_{T(16)}$) of the tubular membrane are calculated on the basis of the cross-section areas of each annulus. The radial conductances ($g_{L(1)}$ to $g_{L(16)}$) between centres of adjacent annuli are also calculated: $g_{L(16)}$ includes the access resistance between the outermost annulus of transverse tubular system and the extracellular fluid. In this way the transverse tubular system is represented by a cable network of sixteen sections. The network resembles the linear cable network used to represent the passive properties of a nerve fibre, with the differences that the network is of finite length and that the elements of which the network is made up (g_T, c_T, g_L) all decrease in value from one section to the next as the fibre axis is approached.

If the potential across the tubular wall (u, sarcoplasmic potential–

potential in tubular lumen) at the centre of the fibre is written as u_1, the potential at the middle of the first annulus as u_2, and the ionic current across the tubular wall of the central disk as i_1 then

$$\frac{du_1}{dt} = \dot{u}_1 = \frac{(u_2 - u_1)g_{L(1)} - i_1}{c_{T(1)}}. \tag{19}$$

Likewise in the first annulus

$$\dot{u}_2 = \frac{(u_3 - u_2)g_{L(2)} - i_2 - (u_2 - u_1)g_{L(1)}}{c_{T(2)}}, \tag{20}$$

and in general for the jth annulus

$$\dot{u}_j = \frac{(u_{j+1} - u_j)g_{L(j)} - i_j - (u_j - u_{j-1})g_{L(j-1)}}{c_{T(j)}}. \tag{21}$$

The ionic currents in eqns. (19)–(21) may be described in a number of ways.

$$i_j = g_{T(j)}(u_j - V'_L), \tag{22}$$

where V'_L is the equilibrium potential for a leak current and $g_{T(j)}$ is a constant conductance. With $V'_L = V_R$ eqn. (22) corresponds to the assumption that the conductance of the tubular wall is linear. Regenerative sodium currents and non-linear potassium currents can be included by defining

$$i_j = g_{T(j)}(u_j - V'_L) + g_{Na(j)}(u_j - V'_{Na}) + g_{K(j)}(u_j - V'_K), \tag{23}$$

where

$$g_{Na(j)} = \bar{g}_{Na(j)} m_j^3 h_j, \tag{24}$$

$$g_{K(j)} = \bar{g}_{K(j)} n_j^4, \tag{25}$$

and m, h, n are Hodgkin–Huxley conductance variables; V'_{Na} and V'_K are the zero-current potentials for the sodium and potassium channels respectively.

The usual first-order equations for m, n, h were used, in which

$$\dot{y} = \alpha_y(1 - y) - \beta_y(y), \tag{26}$$

with the following equations for the rate constants (Adrian *et al.* 1970).

$$\alpha_m = \frac{\bar{\alpha}_m(V - \bar{V}_m)}{1 - \exp(-\frac{1}{10}(V - \bar{V}_m))}, \tag{27·1}$$

$$\beta_m = \bar{\beta}_m \exp(-\tfrac{1}{18}(V - \bar{V}_m)), \tag{27·2}$$

$$\alpha_h = \bar{\alpha}_h \exp(-\tfrac{1}{20}(V - \bar{V}_h)), \tag{27·3}$$

$$\beta_h = \bar{\beta}_h[1 + \exp(-\tfrac{1}{10}(V - \bar{V}_h))]^{-1}, \tag{27·4}$$

$$\alpha_n = \frac{\bar{\alpha}_n(V - \bar{V}_n)}{1 - \exp(-\frac{1}{10}(V - \bar{V}_n))}, \tag{27·5}$$

$$\beta_n = \bar{\beta}_n \exp(-\tfrac{1}{80}(V - \bar{V}_n)). \tag{27·6}$$

The potentials (u_j) within the tubular system can be obtained by the simultaneous numerical solution of the sixteen differential equations for u_j and for i_j. The latter may depend upon differential equations describing the rate of change of m, h and n in each ring. Since

$$I_T = (V - u_{16}) g_{L(16)} \tag{28}$$

one can write from eqn. (3) that

$$\dot{V} = Y, \tag{29}$$

$$\dot{Y} = K\left[Y + \frac{I_1}{C_m} + \frac{(V - u_{16}) g_{L(16)}}{C_m}\right], \tag{30}$$

where

$$I_1 = g_L(V - V'_L) + g_{Na}(V - V'_{Na}) + g_K(V - V'_K) \tag{31}$$

and the g's are for the surface of the fibre and controlled by the usual Hodgkin–Huxley variables m, h and n (Adrian *et al.* 1970).

The equations for i_j, u_j, I_1, V, Y are a set of simultaneous first-order differential equations with independent variable t and can be solved by conventional computer methods. A modified fourth-order Runge–Kutta method as described by Fitzhugh (1966) was used; the actual program being a modification of that used by Adrian *et al.* (1970). It was assumed that the rate constants in the tubular system were the same as in the surface. These rate constants were determined experimentally by a voltage clamp method which, even if perfect, could only control the surface potential (V). They must, therefore, be regarded with caution, and we are aware of the objections to ascribing rate constants determined in this way to surface and tubular membrane separately. However, in the absence of better information it seems a reasonable first approximation.

METHODS

Measurement of action potentials, after potentials and fibre constants were done by conventional micro-electrode methods. The electrotonic potential was measured at three distances from a micro-electrode (at $x = 0$) passing a small constant current into a fibre. The steady-state voltages were plotted semi-logarithmically against the distance from the current electrode (x) and a straight line was fitted by a least-squares method. The length constant ($\lambda = \sqrt{(r_m/r_i)}$) and the input resistance ($\frac{1}{2}\sqrt{(r_m r_i)}$) were obtained from the slope of the line and the voltage and current at $x = 0$. The equivalent radius of each fibre examined was calculated from r_i assuming circular cross-section and a value for the sarcoplasmic specific conductivity of 5·9 mho cm^{-1} (Hodgkin & Nakajima, 1972*a*).

After making the recordings of electrotonic potential two recording electrodes were left in the fibre close to and a few millimetres from the current electrode. A brief current was passed through the current electrode in order to stimulate the fibre. The conduction velocity was measured from the delay between the action potentials at the two recording positions.

Calculation of propagated action potentials

The calculation of the propagated action potential was started by assuming a value of the propagation velocity θ and from it the propagation constant K was computed ($R_i = 169\ \Omega$ cm). Eqn. (18) was then solved for μ. ΔV was taken as 0·1 mV and Δu_j at appropriate radii were calculated by eqns. (14) and (16). Using these initial values, currents (i_j) and potentials for each annulus (u_j) and for the surface (V) were computed for $t > 0$. If K is chosen too high the calculated V goes to $+\infty$ and if too low V goes to $-\infty$. The program was arranged so that a single calculation was ended if $V > V'_{Na}$ or $V < V'_K$; K was interpolated between values which gave solutions diverging in opposite directions and the solution restarted until K was determined to within 1 bit in 36 (approximately 1 part in 7×10^{10}). This procedure calculates the spike of the action potential and the beginning of the after potential. For the remaining part of the after potential successive iterations using the interpolation procedure described by Fitzhugh & Antosiewicz (1959) were used.

Calculation of voltage clamp currents

The calculation of currents during voltage clamp experiments proceeded as above except that the surface potential was held fixed and longitudinal propagation was not considered. The tubular annuli were treated in the same way as above, with currents (i_j) and potentials (u_j) computed at various times greater than zero. The input current is then the sum of the current through the surface element and that through R_s.

Computing

Programs were written in Fortran and computations were done on the Atlas 2 (Titan) computer at the Computer Laboratory in Cambridge, and on the PDP 6 computer at the Medical School Computer Facility of the University of Pennsylvania (National Institutes of Health Grant, No. RR-15).

RESULTS

Fig. 1 shows calculations of propagated action potentials for three fibres of different radii at 20° C. Table 1 gives in detail the numerical values of the constants used for these calculated action potentials. The most relevant points are that the kinetic parameters for the membrane of the fibre surface are essentially similar to those used by Adrian *et al.* (1970) for calculations with a passive, lumped tubular system. Some small changes have been made in order to increase the propagation velocity, which is reduced when the T-system is considered to be distributed. In particular the specific capacitance of the surface and tubular membrane has been set at $0{\cdot}9\ \mu$F cm^{-2} (Hodgkin & Nakajima, 1972*b*); $\bar{\alpha}_m$ has been increased from 0·04 to 0·046: the saturating sodium conductance of the surface ($\bar{g}_{Na}$) has been increased from 145 mmho cm^{-2} at 20° C to 180 mmho cm^{-2}. The zero-current potential of the delayed current channel (V'_K) has been taken as -85 mV. Adrian *et al.* (1970) used a value of -70 mV (see below). In Fig. 1 the access resistance R_s has a value of $150\ \Omega$ cm^2 and the saturating sodium conductance of the

TABLE 1*A*. Values of Hodgkin–Huxley rate constants at 2° C and zero-current potentials

(1)	(2)	(3)	(4)	(5)
$\bar{\alpha}_m$	0·016, 0·042 msec^{-1}	0·04	0·046	0·04
$\bar{\beta}_m$	0·16, 0·42 msec^{-1}	0·4	0·4	0·4
$\bar{V}_m$	−40 to −48 mV	−42	−42	−42
$\bar{\alpha}_h$	0·003 msec^{-1}	0·003	0·003	0·003
$\bar{\beta}_h$	0·65 msec^{-1}	0·65	0·65	0·65
$\bar{V}_h$	−41 mV	−41	−41	−41
$\bar{\alpha}_n$	0·0021–0·0044 msec^{-1}	0·0044	0·0044	0·004
$\bar{\beta}_n$	0·009–0·0185 msec^{-1}	0·01848	0·01848	0·01848
$\bar{V}_n$	−40 to −45 mV	−40	−40	−40
V'_{Na}	+15 to +22 mV	+50	+50	+50
V'_K	−70 to −85 mV	−70	−85	−85
V'_L	−95 mV	−95	−95	−95

Columns (2) and (3) are from Adrian *et al.* (1970) and are respectively the experimental values and the values used by them in reconstructing the action potentials. The experimental values were obtained from fibres in Ringer plus 350 mM sucrose at 1–3° C, and the values for V'_K and V'_{Na} used in computations are estimated for isotonic Ringer fluid to correct for hypertonicity.

Column (4) are the values of the rate constants at 2° C used to reconstruct the action potentials in this paper. To calculate the rate constants at 20° C a Q_{10} of 2·5 was used.

Column (5) are the values of the rate constants at 2° C used to reconstruct the voltage clamp potentials and currents in this paper. A Q_{10} of 2·5 was used to obtain the rate constants at 20° C.

B. Electrical constants for surface and tubular membranes

Surface constants: these are given for a square centimetre of surface membrane at 20° C

	(1)	(2)
Leak conductance (g_L)	0·24 mmho cm^{-2}	0·24 mmho cm^{-2}
Limiting sodium conductance ($\bar{g}_{Na}$)	180·0 mmho cm^{-2}	145·2 mmho cm^{-2}
Limiting potassium conductance ($\bar{g}_K$)	41·5 mmho cm^{-2}	41·5 mmho cm^{-2}
Capacitance (C_m)	0·9 μF cm^{-2}	1·0 μF cm^{-2}
Access resistance (R_s)	150 Ω cm^2	150 Ω cm^2

Tubular constants: these are given for a square centimetre of tubular membrane at 20° C

Leak conductance	0·0067 mmho cm^{-2}	0·0067 mmho cm^{-2}
Limiting sodium conductance	9·0 mmho cm^{-2}	9·0 mmho cm^{-2}
Limiting potassium conductance	1·27 mmho cm^{-2}	1·27 mmho cm^{-2}
Capacitance (C_w)	0·9 μF cm^{-2}	1·0 μF cm^{-2}

Column (1) refers to calculated action potentials: Column (2) to calculated voltage clamp currents and potentials.

tubular membrane expressed per square centimetre of that membrane is 9 mmho cm^{-2} at 20° C, that is one-twentieth of the value in the surface membrane. The specific saturating potassium and leak conductances of the tubular membrane were 1/33 and 1/36 times the values in the surface membrane respectively. Values for the geometrical constants of the tubular system are the same as those used in Adrian *et al.* (1969).

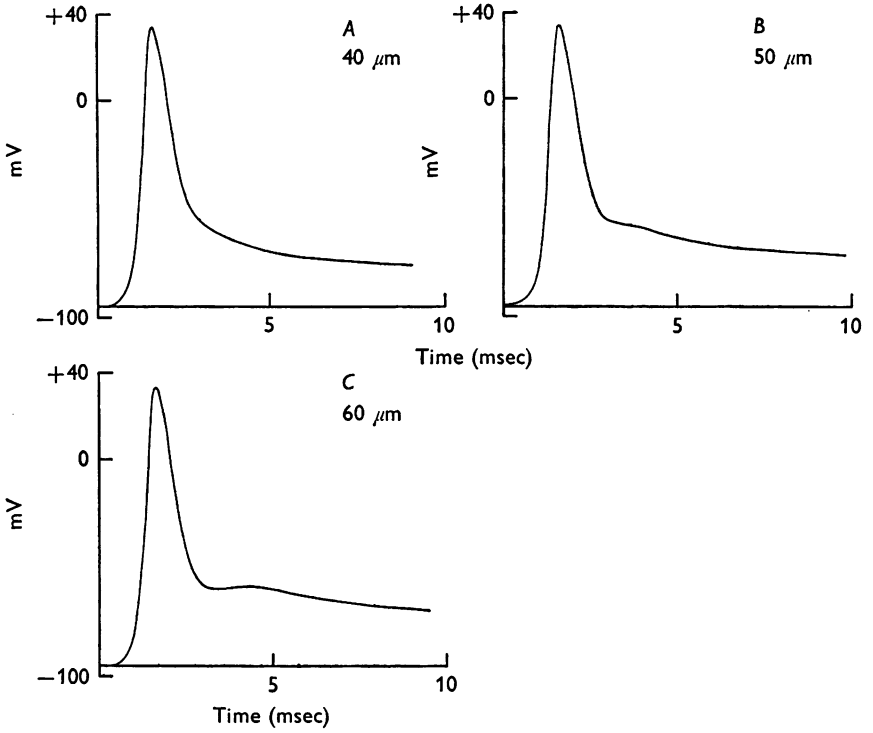

Fig. 1. Propagated action potentials calculated for muscle fibres of different diameter. Temperature 20° C. *A*, fibre radius 40 μm; *B*, fibre radius 50 μm; *C*, fibre radius 60 μm. Numerical values used for these calculations are in Table 1 and in the text.

Fig. 1 *A* shows an action potential for a fibre of radius 40 μm. The after potential declines monotonically. In Fig. 1 *B* the after potential shows the beginnings of a step and in 1 *C* there is a definite positive-going hump to the after potential. The radius for 1 *B* and 1 *C* are 50 and 60 μm respectively.

A humped after potential frequently is seen in records of action potentials from frog striated muscle fibres. However, only monotonically declining after potentials were obtained in the reconstructions of the action potential using the simpler two-time constant model (Adrian *et al.* 1970). In the

present model, which is a 17 time constant model, the hump is still present, though reduced in size, when the electrical properties of the tubular network are assumed to be linear; when $\bar{g}_{Na(j)}$ and $\bar{g}_{K(j)}$ are zero (see Table 2). The hump occurs because the surface of the fibre repolarizes while the tubular

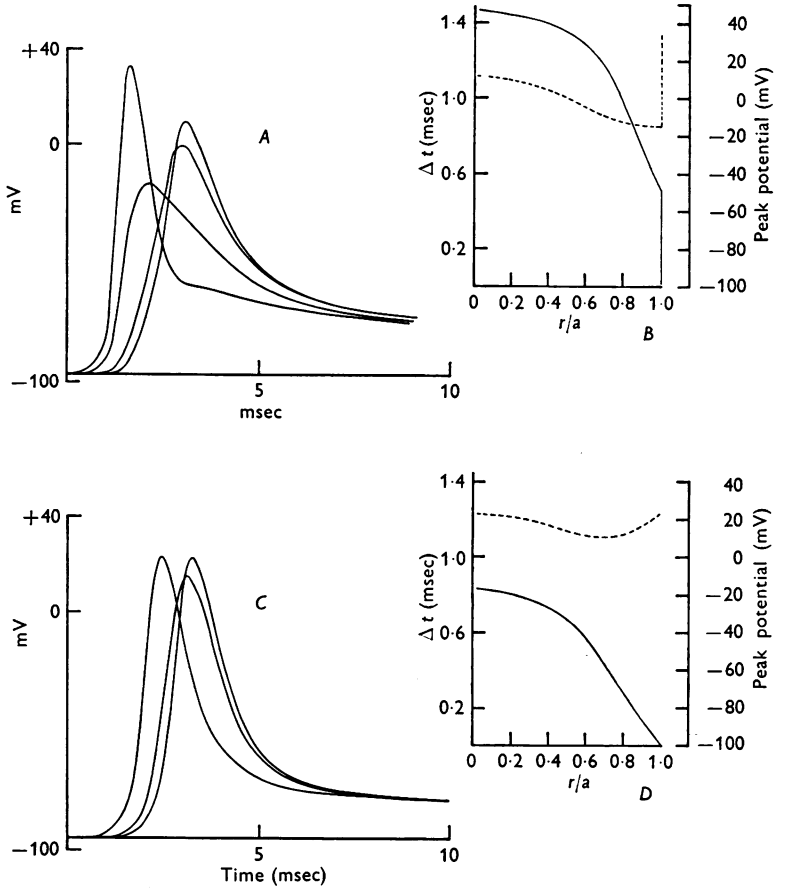

Fig. 2. Calculated action potentials in a fibre with a radius of 50 μm at 20° C (see also Figs. 1*B*, 4, 6). *A* and *B*: numerical parameters as in Fig. 1*B*. *A*: propagated action potential across fibre surface, potential change just inside access resistance, half-way to the axis of the fibre, and at the fibre axis. *B*: the interval (Δt) between the peak of the surface action potential and the peak of the potential change as a function of radial position; and the magnitude (dashed line) of the potential change as a function of radial position. *C* and *D*: numerical parameters as in *A* and *B* but with no access resistance ($R_s = 0$). *C*: propagated action potential, potential changes half-way to and at the fibre axis. *D* as *B* above. Note how the access resistance attenuates the surface potential change at the outer border of the tubular system, and delays the peak potential changes in the tubular system.

system is still depolarized. During this period following the spike, the surface of the fibre is supplying some of the current to recharge the tubular capacity and the conductance of the surface potassium channels, which provide this current, is decreasing. Plainly the interactions of the surface and tubules are complex, but in general it is reasonable that with a larger fibre diameter, the effect of the tubules should be larger, delayed, and continue for longer. In the small fibres the depolarizations of the surface and tubules are more nearly synchronous so that the current for repolarizing the tubules is taken earlier when the potassium conductance of the surface is still high.

Fig. 2*A* shows in greater detail the action potential in the fibre with a radius of 50 μm (see also Table 2, line 2). It shows the potential across the surface of the fibre, which is the potential change that would be recorded with a micro-electrode, the potential change across the tubular wall just inside the access resistance, the potential change half-way along the fibre radius ($r/a = 0{\cdot}5$) and the potential change at the axis of the fibre. Fig. 2*B* shows the interval between the peak of the potential change at any radial distance and the surface potential peak. It clearly shows that the radial potential change does not propagate at a constant velocity. Fig. 2*B* also shows (dashed line) the peak potential change at any radial distance. Fig. 2*C* shows the surface action potential and tubular changes for $r/a = 0{\cdot}5$ and for $r = 0$. These are calculated with the same parameters as Fig. 2*A* with the single difference that the access resistance is zero ($R_s = 0$; see also Table 2, line 4). Fig. 2*D* shows the radial conduction time and the peak potential change as functions of the radius. In the absence of any access resistance the potential change in the surface and in the outermost annulus of the tubular system are practically identical. Removing the access resistance slows the longitudinal conduction velocity, reduces and broadens the action potential, and greatly affects the configuration of the after potential. In general the interaction of the surface and the tubules is greater in the absence of any access resistance.

Table 2 gives values of various measurements from calculated action potentials including those in Figs. 1 and 2. The first three lines show the effect of fibre diameter. Lines 4 to 8 show the effects of increasing access resistance. The last three lines of the table show the effects of altering the tubular sodium conductance. In Table 2 the total capacity is the surface and tubular capacity calculated per square centimetre of fibre surface on the basis of the tubular geometry and a specific capacity of 0·9 μF cm^{-2}:

$$\text{total capacity} = 0{\cdot}9(1+\rho a/2\zeta).$$

The measurable capacity at zero frequency is the capacity that is measured by integrating the transient current which flows when the fibre surface is made to undergo a step change in potential. The measurable resistance is

TABLE 2. Calculated fibre constants and action potential properties

Radius a (μm)	Access resistance R_s (Ω cm^2)	Lumen conductance G_L (mmho cm^{-1})	Limiting ionic conductances mmho cm^{-2} fibre surface				Capacity (μF cm^{-2})		Measurable capacity (μF cm^{-2})	Resistance (Ω cm^2)	Propagation velocity		Peak centre potential (mV)	Hump (mV)
			$\bar{g}_{Na}$	$\sum_1^{16}\bar{g}_{Na(j)}$	$\bar{g}_K$	$\sum_1^{16}\bar{g}_{K(j)}$	Total	C_t			Longitudinal (cm sec^{-1})	Radial (cm sec^{-1})		
40	150	10	180	54·0	41·5	7·6	6·30	1·80	6·21	3452	180·5	3·6	+14	—
50	150	10	180	67·5	41·5	9·5	7·65	1·81	7·49	3338	200·5	3·3	+11	—
60	150	10	180	81·0	41·5	11·4	9·00	1·82	8·76	3235	218·8	3·2	+8	1
50	0	10	180	67·5	41·5	9·5	7·65	3·98	7·59	3334	109·5	6·2	+23	—
50	50	10	180	67·5	41·5	9·5	7·65	2·76	7·56	3335	144·3	4·5	+19	—
50	150	10	180	67·5	41·5	9·5	7·65	1·81	7·49	3338	200·5	3·3	+11	—
50	250	10	180	67·5	41·5	9·5	7·65	1·49	7·43	3341	233·9	2·5	−5	10
50	150	20	180	67·5	41·5	9·5	7·65	1·93	7·52	3339	190·7	4·6	+10	—
50	150	10	180	0	41·5	0	7·65	1·81	7·49	3338	200·5	3·6	−47	0·1
50	150	10	180	42·2	41·5	9·5	7·65	1·81	7·49	3338	200·5	3·1	−10	—
50	150	10	180	84·5	41·5	9·5	7·65	1·81	7·49	3338	200·5	3·6	+21	—

the resistance which would be measured from the fibre length constant and the input resistance:

$$\text{measurable capacity} = 0{\cdot}9\left\{1+\frac{\rho a}{2\zeta}\left(\frac{I_0^2(\nu a)-I_1^2(\nu a)}{\{I_0(\nu a)+R_s\bar{G}_L\nu I_1(\nu a)\}^2}\right)\right\}\mu\text{F cm}^{-2},$$

$$\text{measurable resistance} = \left\{g_L+\frac{\nu\bar{G}_L I_1(\nu a)}{I_0(\nu a)+R_s\bar{G}_L\nu I_1(\nu a)}\right\}\Omega\,\text{cm}^2$$

(for discussion of these relations see Hodgkin & Nakajima, 1972*b* and Peachey & Adrian, 1973).

The capacity from the foot of the action potential is derived from the propagation velocity (θ) and the rate constant (μ) for the exponential rise of the action potential.

$$C_f = \frac{\mu a}{2\theta^2 R_i}$$

R_i was taken to be 170 Ω cm ($G_i = 5{\cdot}9$ mmho cm^{-1}). This relationship assumes that the capacitative current during the foot of the action potential is much greater than the ionic current. The longitudinal propagation velocity is the value used in the computation of the action potential, and the radial propagation velocity is taken as the fibre radius divided by the time between the peaks of the potential change at the surface and the centre of the fibre. The final column 'after potential hump' is the voltage change from the minimum immediately following the spike, to the maximum of the after potential. A dash in this last column means that at all times after the spike $dV/dt \leqslant 0$.

The results given in Table 2 and in particular the effects of tubular sodium currents and of the access resistance (R_s) are most easily shown by Figures. In Figs. 3–6 we have plotted four calculated action potentials using a three-dimensional surface whose co-ordinates are potential, time and distance from the axis of the fibre. Figs. 3–6 plot the time courses of potential change at various radial distances: the individual potential-time curves are what would be recorded between an electrode in the sarcoplasm and an electrode in the tubular lumen at the indicated radial position.

In all four Figures the fibre diameter is 100 μm; the total capacity is 7·65 μF cm^{-2}; the conductivity of the tubular lumen (G_L) is 10 mmho cm^{-1}. The geometric constants of the tubular system are the standard values used in all the calculation of this paper ($\rho = 0{\cdot}003$; $\zeta = 10^{-6}$ cm; $\sigma = 0{\cdot}5$). The saturating sodium and potassium conductances of the fibre surface ($\bar{g}_{Na}$ and $\bar{g}_K$) are respectively 180 mmho cm^{-2} and 41·5 mmho cm^{-2} and the temperature is taken as 20° C.

Fig. 3 shows the prediction for a passive tubular system and no access resistance: that is $R_s = 0$ and the tubular membrane current is given by

eqn. (22). In this reconstruction the action potential rises and falls slowly and propagates at only 109 cm sec^{-1}. Neither of these faults is improved by adding sodium and potassium conductance to the tubes as in Fig. 4. In this reconstruction the tubular membrane currents are given by eqn. (23). The longitudinal propagation velocity is still 109 cm sec^{-1}. Figs. 3 and 4 suggest that it is the capacity of the tubular system which slows the surface potential change. A substantial reduction of the tubular capacity would increase the propagation velocity. However, Hodgkin & Nakajima (1972*a*) suggest that 7·65 μF cm^{-2} is an appropriate value for a fibre with a diameter of 100 μm.

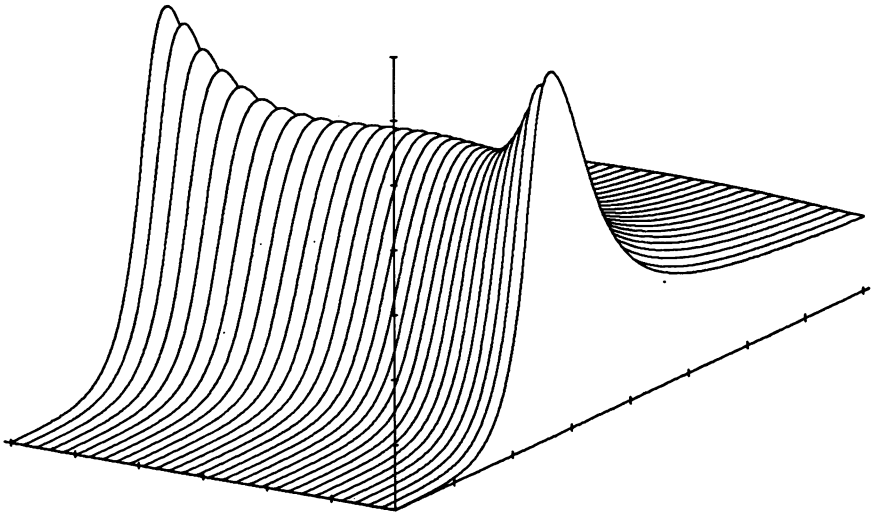

Fig. 3. Calculated action potential in a fibre with a radius of 50 μm. The access resistance to the tubular system (R_s) is zero and the ionic current in the tubular wall is linear (eqn. (22)). There are no activatable ionic currents in the tubular membrane. The calculated propagation velocity is 109 cm sec^{-1}. The three co-ordinates are: vertical, potential in 20 mV divisions; horizontal, the fibre diameter divided into six equal divisions; horizontal (receding), time in 1 msec divisions.

Alternatively a substantial increase in $\bar{g}_{Na}$ would increase the rate of rise of potential and the propagation velocity, but there is little evidence that $\bar{g}_{Na}$ has been grossly underestimated. Ildefonse & Roy (1972) suggest a value of 50 mmho cm^{-2} for $\bar{g}_{Na}$. This value is substantially less than the estimate of Adrian *et al.* (1970) which is the basis for the figure used in the present calculations. We have, therefore, chosen to diminish the effects of tubular capacity on the surface potential by introducing a resistance between the surface and the tubular lumen. Fig. 5 shows the calculated action potential for passive tubules (eqn. (22)) and an access resistance (R_s) of 150 Ω cm^2. The access resistance makes little difference to the measurable membrane

resistance and capacity (see Table 2, lines 2 and 4) but the rates of rise and repolarization are now reasonably rapid and the propagation velocity is 200 cm sec^{-1}. The addition of tubular sodium and potassium conductances (Fig. 6) once again does not change the longitudinal propagation velocity but does increase the axial potential change.

The four action potentials in Figs. 3–6 differ in only two features: the presence and absence of the access resistance and the presence and absence of activatable sodium and potassium conductances in the tubular system.

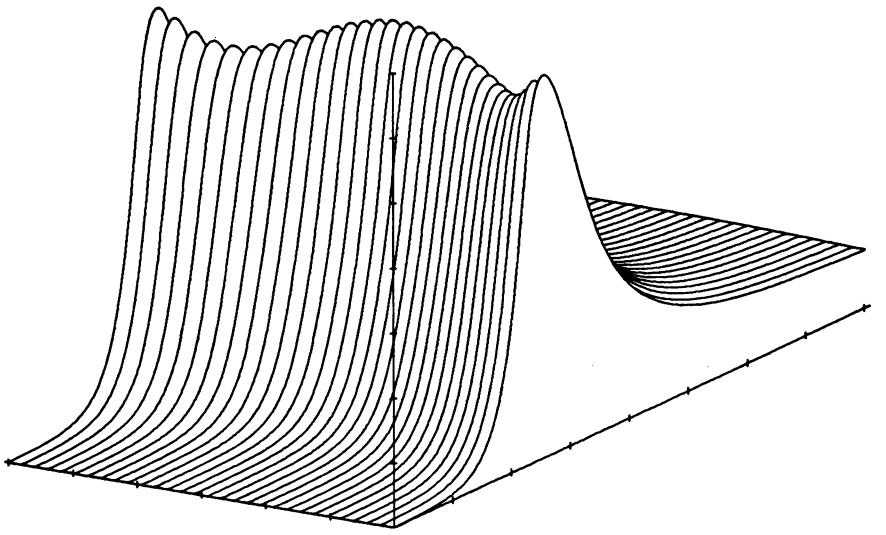

Fig. 4. Calculated action potential for a fibre with a radius of 50 μm. The access resistance is zero and there are activatable sodium and potassium currents in the tubular wall (eqn. (23)). The calculated propagation velocity is 109 cm sec^{-1}. See line 4 of Table 2. Scaling of axes as in Fig. 3.

Of these calculated action potentials, the one shown in Figs. 2 *A* and 6 is the best replica of experimentally recorded action potentials. We do not know whether other geometries or combinations of parameters would do as well or better.

The model used for calculation allows a wide choice of parameters and some additional justification should be given for the choices made in Fig. 1. The conductances for the surface membrane are close to those used by Adrian *et al.* (1970), and we are, therefore, assuming that the total *measurable* limiting sodium and potassium conductances are appropriate values to use for the conductance of the surface (see below).

The tubular lumen conductance (G_L), access resistance to the tubular system (R_s), tubular limiting sodium ($\bar{g}_{Na(j)}$) and tubular limiting potassium conductance ($\bar{g}_{K(j)}$) all have substantial effects on the configuration of the

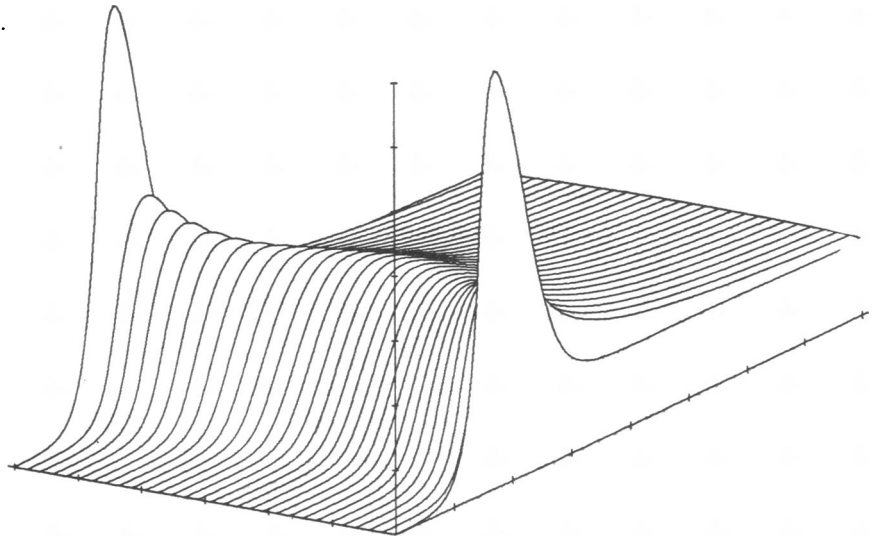

Fig. 5. Calculated action potential for a fibre with a radius of 50 μm. The access resistance to the tubular system (R_s) is 150 Ω cm^2 and the ionic current in the tubular wall is linear (eqn. (22)). The calculated propagation velocity is 200 cm sec^{-1}. See line 9 of Table 2. Scaling of axes as in Fig. 3.

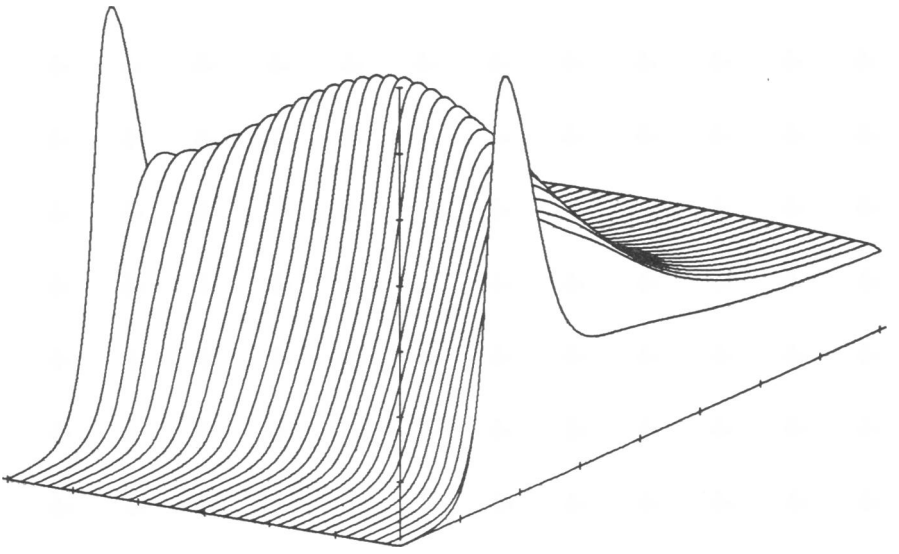

Fig. 6. Calculated action potential for a fibre with a radius of 50 μm. The access resistance is 150 Ω cm^2 and there are activatable sodium and potassium currents in the tubular wall (eqn. (23)). The calculated propagation velocity is 200 cm sec^{-1}. See line 2 of Table 2. Scaling of axes as in Fig. 3.

after potential. Decreasing G_L delays and reduces the hump. Increasing R_s increases the size of the hump both by raising the potential at its maximum and by deepening the notch which precedes the hump. Increasing $\bar{g}_{Na(j)}$ increases the potential at the plateau or peak of the after potential and may fill in the notch before the after potential (Fig. 7). The values of $\bar{g}_{K(j)}$ mainly affect the speed of repolarization of the after potential.

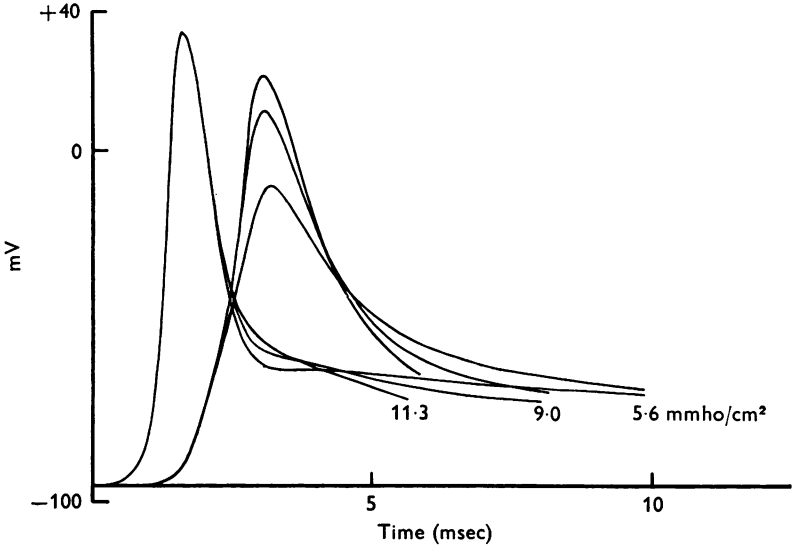

Fig. 7. Calculated surface and axial action potentials using three values for the saturating sodium conductance in the tubular membrane, and otherwise the same constants as the action potential in Figs. 1 and 6. The three values of the sodium conductance are lower than, equal to, and larger than the standard value, 5·6, 9·0, and 11·3 mmho cm^{-2}. The tubular sodium conductance affects the shape of the after potential and the maximum depolarization at the fibre axis.

There are other constraints which can be used to guide the choice of values for various parameters. Lines 4–7 in Table 2 show the effects of the access resistance on the measurable low- and high-frequency capacities, the longitudinal and radial propagation velocity and the peak of the potential change at the centre of the fibre. The action potentials in Fig. 1 are calculated for an access resistance of 150 Ω cm^2. In a fibre with a radius of 50 μm this gives a conduction velocity of 200·5 cm sec^{-1}, a time constant for the foot of the action potential ($1/\mu$) of 200 μsec, and a capacity from the action potential foot (C_f) of 1·81 μF cm^{-2}. The corresponding average figures from Hodgkin & Nakajima (1972*b*) are 209 cm sec^{-1}, 127 μsec, and 2·59 μF cm^{-2}. The value of R_s chosen in Fig. 1 represents a compromise. Increasing it beyond 150 Ω cm^2 would increase the conduction velocity but make the after

potential implausibly large and decrease the value of C_f. Reducing R_s below 150 Ω cm^2 reduces the conduction velocity but increases C_f.

Gonzalez-Serratos (1971) has measured the radial propagation velocity of activation during a twitch and finds it to be 7 cm sec^{-1} at 20° C. This implies that the activation at the centre of a 60 μm fibre should lag the surface activation by just less than 1 msec. If one can assume that the moment of contraction follows the peak potential after a fixed interval, the radial propagation velocity of activation suggests a maximum separation of the peaks of the potential change at the surface and the centre of the fibre. This separation is mainly controlled by the dimension of the tubular system, the conductance of the tubular lumen (G_L) and the capacity of the tubular wall (C_W). We have made the same assumptions about the tubular geometry as were made by Adrian, Chandler & Hodgkin (1969). Decreasing the luminal conductance below 10 mmho cm^{-1} increases the lag of the axial potential on the surface potential. Conversely, increasing this conductance decreases the lag (line 8, table 2). The radial velocities in Table 2 are all less than the measurement of Gonzalez-Serratos, and this must be considered a serious deficiency of the proposed model, or of our assumed relation between contraction and potential.

The magnitude of the axial potential excursion depends very largely on the magnitude on the limiting sodium conductance ($\bar{g}_{Na(j)}$) in the tubules. The last 3 lines in Table 2 show that the tubular sodium conductance has little effect on the longitudinal conduction velocity but a large effect on the peak potential at the centre of the fibre. If the tubular conductance is linear (eqn. (22)), then the centre of the tubular system is not depolarized beyond about -45 mV. Though the rheobase depolarization is exceeded at the centre of the fibre, activation might not occur because the depolarization is not maintained for long enough (Adrian, Chandler & Hodgkin, 1969). If the axial potential is to reach 0 mV, the limiting sodium conductance of unit area of tubular wall needs to be about a twentieth of the limiting sodium conductance of the surface. This implies that for each square centimetre of fibre surface the associated tubular system has a total limiting sodium conductance which is about two thirds of the conductance in the surface.

Measurement of the after-potential

In all calculations it was clear that the fibre diameter was an important variable for the appearance of the after potential hump. Experimentally we were unable to show such a clear dependence. We measured the length constant (λ) and the input resistance of forty-eight fibres from seven sartorius muscles in a Ringer solution at 20° C (Adrian, 1956). From these measurements and a value of 5·9 mmho cm^{-1} for the specific resistance of the sarcosplasm, the radius of each fibre was determined. After measuring

the fibre constants, each fibre was stimulated via the current passing electrode, and the action potential was recorded by two internal micro-electrodes separated by several mm. Fig. 8 shows the after potentials recorded from the distal electrode (for reasons of space the spike of each

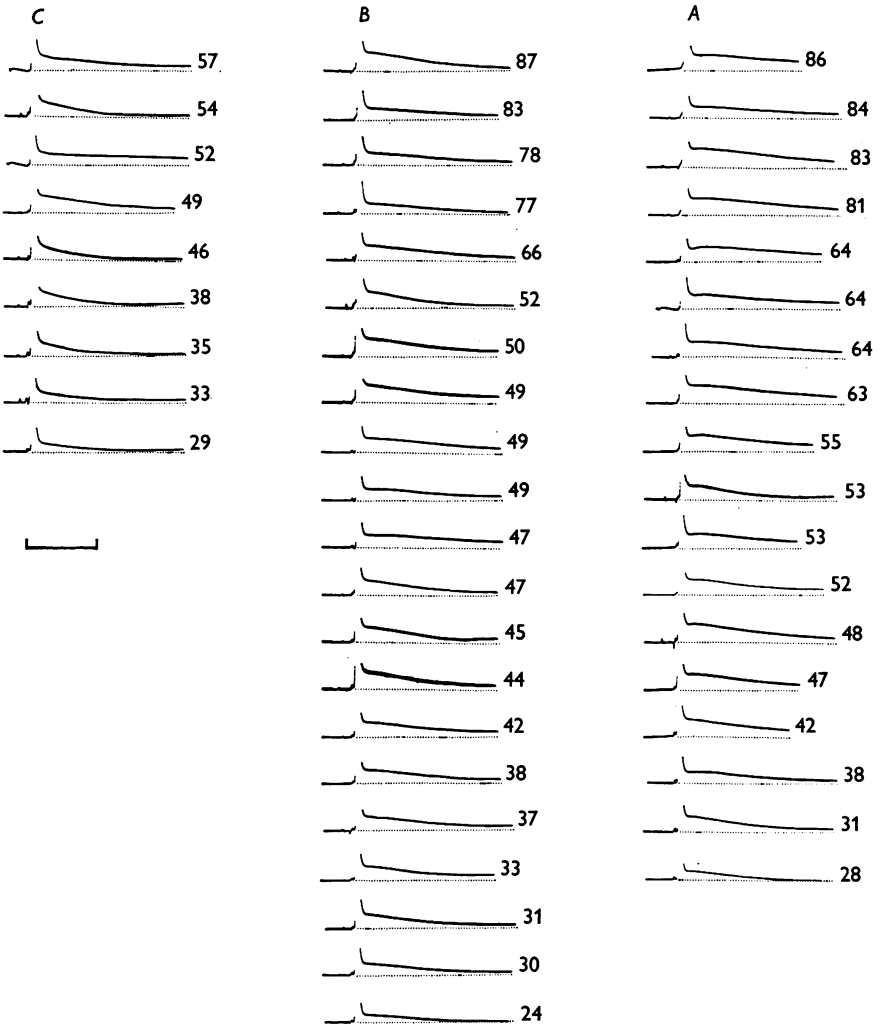

Fig. 8. Experimentally recorded after-potentials in frog sartorius fibres at 20° C. The spike of each action potential has been erased. The number at the end of each record is the radius of fibre estimated from the internal longitudinal resistance (r_i). *A*: fibres where dV/dt is always negative after the spike of the action potential. *B*: fibres where $dV/dt \cong 0$ during the after-potential. *C*: fibres where $dV/dt > 0$ during the after-potential. The horizontal line is 20 msec long.

record has been omitted). The records have been grouped by eye into three groups; those where dV/dt is always negative after the spike of the action potential; those where dV/dt approaches close to zero; those where $dV/dt > 0$ at some time following the spike. The number at the end of each record indicates the radius of each fibre in microns. Table 3 summarizes some measurements on these groups of fibres. The after potentials in which $dV/dt > 0$ (group A) come from fibres whose average diameter is greater than the average diameter of the group where $dV/dt < 0$ (*C*), but an analysis of variance (*f* test) shows that the differences in the diameter of the three groups are not significant at the 5 % level. If there is a correlation of diameter and hump in the after potential, it is obscured by other factors which are unrelated to diameter but which affect the shape of the after potential. Variability of R_s, tubular lumen conductance, and the tubular limiting sodium conductance are examples of such factors which, on the basis of the calculated action potentials, could override the effect of diameter.

TABLE 3. Measured fibre characteristics of fibres with different shapes of after potential

Fibre group	Radius μm	R.P.* mV	R_m Ω cm^2	No.	Potential of peak or plateau mV
All	$51{\cdot}8 \pm 2{\cdot}5$	$-79{\cdot}5$	2156 ± 55	48	—
A	$57{\cdot}6 \pm 4{\cdot}1$	$-79{\cdot}2$	2187 ± 98	18	$-63{\cdot}9 \pm 0{\cdot}9$
B	$50{\cdot}4 \pm 3{\cdot}8$	$-80{\cdot}1$	2216 ± 87	21	
C	$43{\cdot}7 \pm 3{\cdot}3$	$-78{\cdot}6$	1952 ± 60	9	—

Time to maximum of after potential in Group A fibres from upstroke of action potential $5{\cdot}6 \pm 0{\cdot}2$ msec.

Average conduction velocity of all fibres 256 cm/sec.

* Measured on photograph of action potential – not on initial electrode penetration.

Effect of distributed tubular parameters on voltage clamp currents

At first sight the assignment to the tubular system of a limiting sodium conductance only slightly less than the limiting sodium conductance of the surface, might seem inconsistent with the assumption that the total measurable limiting sodium conductance should be assigned to the fibre surface.

There are several reasons why this is not so. First, the presence of an access resistance will limit the contribution of the tubular sodium conductance to the measurable sodium current. Secondly, the tubular sodium conductance develops at a later time than the surface sodium conductance and, therefore, the peak measured sodium current is not increased in proportion to the additional tubular sodium conductance. Thirdly, during the first few msec of a depolarizing voltage step, redistribution of the charge on the

tubular capacity produces a transient outward current which diminishes the peak inward current.

To illustrate these effects quantitatively voltage clamp currents have been calculated using the same model as for the calculations of the action potentials. The command step of potential is imposed on the element of the cable representing the surface; currents are calculated for that element, assuming that the surface capacity is charged instantaneously. The voltages and currents in the sixteen elements of the cable are calculated by the same set of simultaneous differential equations as are used in the action potential calculation. The current required to hold the surface element to the required potential is then the current in that element plus the current delivered to the tubular system via the access resistance R_s. The presence of this resistance acts to increase the independence of the tubular system from the clamping system. In any actual clamping experiment on a muscle fibre, the recorded current will therefore be a complex mixture of surface and tubular capacity currents and surface and tubular ionic currents. This mix will not be a constant one, since regenerative currents in the tubular system may radically alter the shape of the potential profile across the fibre at different depolarizations of the fibre surface.

The complexities described below are by no means confined to muscle fibres and would be expected in any situation where a part of the membrane generating current is separated by an external or internal resistance from the part of the membrane whose potential is being measured and controlled. The regular geometry of the tubular system makes it reasonably straightforward to represent its morphology in cable elements.

How far is one misled by supposing that the current required to clamp the surface with its attached tubules is the current passing across a membrane consisting of a capacity, a leak, a sodium system (m, h), and a potassium system (n)? Adrian *et al.* (1970) made this assumption in their analysis of the voltage clamp currents of striated muscle fibres. The major source of error is neglect of the tubular capacity current. Neglecting the tubular sodium current makes surprisingly little difference.

Figs. 9 and 10 show calculated voltage clamp experiments. The constants used in these calculations differ in some minor respects from the constants used for the action potentials. They are shown in column (5) in Table 1*A*. The calculations are for a fibre with a diameter of 120 μm. The tubular sodium and potassium conductances are similar to those used for the action potential calculations. The access resistance, tubular geometry and passive tubular properties are the same. On the left are the command potentials, left of centre, the current in the surface element, right of centre the total required current, and on the right the potential at the centre of the fibre. It is immediately apparent that the current records, though they differ in

detail, show no major quantitative differences, even when the centre of the fibre differs substantially in potential from the surface. Fig. 11 plots the early currents for the surface element alone and for the surface with the tubular elements. The sodium conductances measured by the slopes of the current at the apparent V'_{Na} are not very different (71 mmho cm^{-2} from surface, 72 mmho cm^{-2} from total). The chief difference is in the size of the early currents. Also the zero-current potential for the sodium channel (V'_{Na}) which is set to be +50 mV in these calculations, would be incorrectly esti-

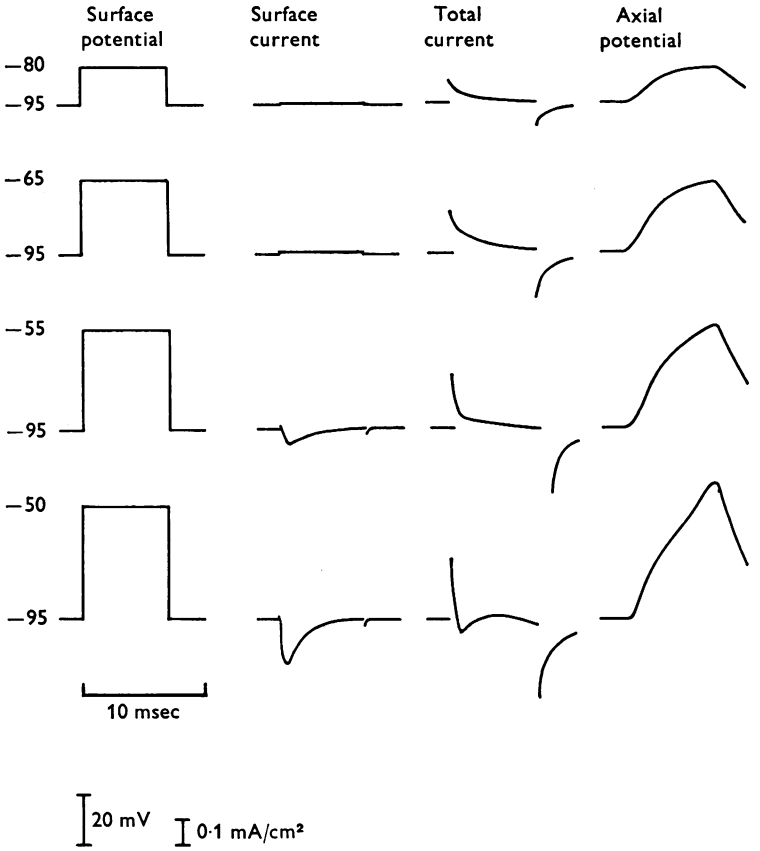

Fig. 9. Calculated total current and surface current in a voltage clamp. Each set of calculations shows from left to right, the command potential at the surface of the fibre, the current through the surface, the total current delivered to the fibre surface and to the tubular system, the potential across the tubular wall at the axis of the fibre. The changing of the surface capacity takes place instantaneously so no capacitative transient is seen in the surface current. When the surface potential is taken to −55 mV, the axial potential depolarizes by a few mV more than −55 mV (cf. Costantin, 1970). Temperature 20° C; fibre radius 60 μm; numerical values in Table 1.

mated from the total current to be +42 mV. An exactly similar effect of tubular capacitative current is shown in Fig. 12 on the zero-current potential for the potassium system (V'_K). Fig. 12*A* shows tail currents after a return of the command potential from 0 mV to various potentials. The value of V'_K incorporated into the calculations is −85 mV and it can be seen that the current in the surface element, as expected, is unchanging when

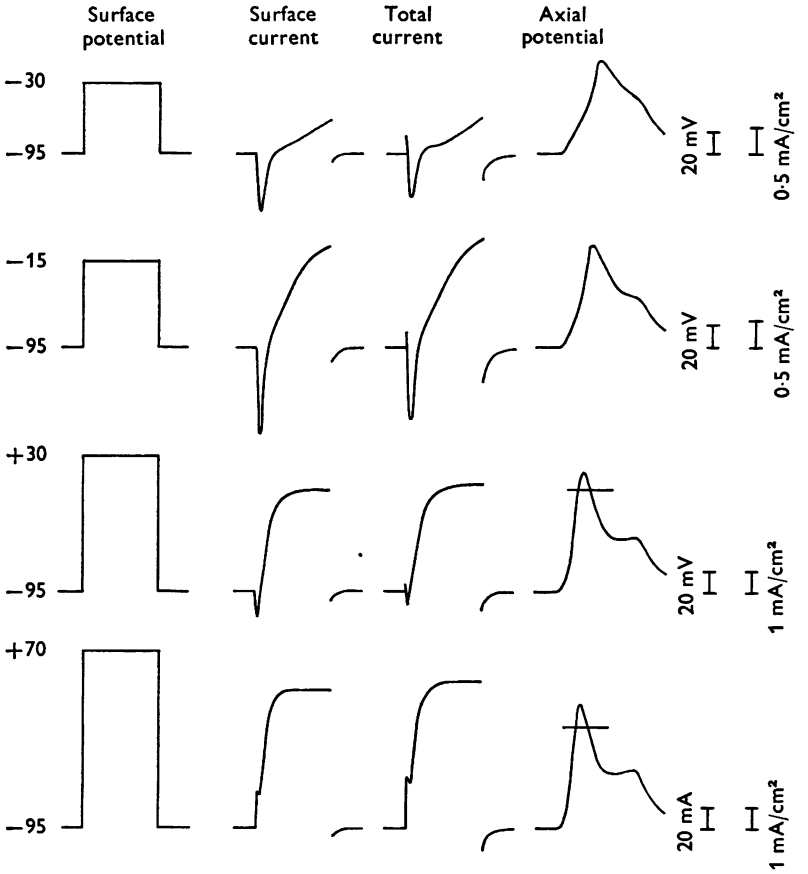

Fig. 10. Calculated currents and axial potential during a voltage clamp for depolarizations into the region of 0 mV and beyond V'_{Na}. Conditions are the same as Fig. 8.

the command potential returns to −85 mV. However, when the total currents are considered there is still a considerable inward transient current on returning to −85 mV. The best estimate of a zero-current potential from the total currents would be −80 mV. Adrian *et al.* (1970) estimated V'_K to be −70 to −75 mV at 20° C and there is a suggestion in their Table 4 that at

2° C V'_K was 10 or 15 mV more negative. This effect is to be expected if the estimate of V'_K is in error because of capacitative tubular currents. In the cold when the rate constant for the deactivation of n will be much reduced, the tail currents would outlast the capacitative currents and could be seen in a less adulterated form. Fig. 12*B* shows tail currents calculated at 2° C (Q_{10s} for rate constants = 2·5). Though there is still a large contribution of tubular capacity current the best estimate of V'_K would be close to − 85 mV.

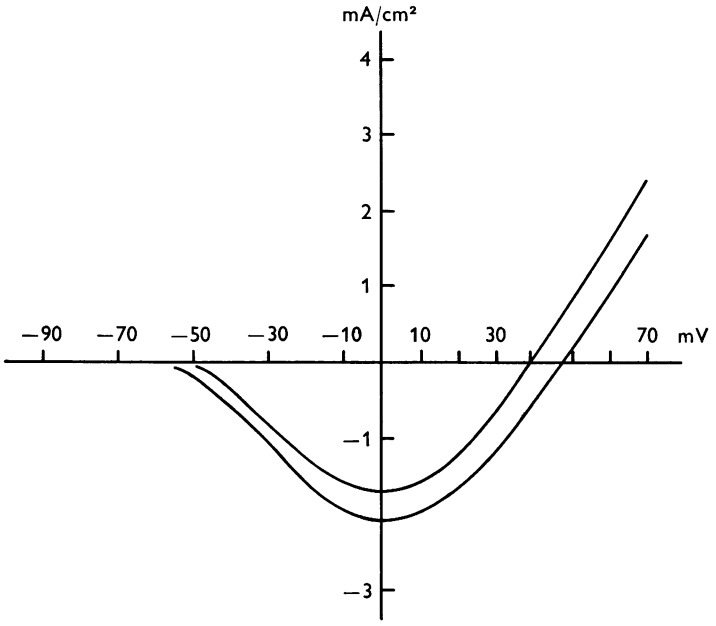

Fig. 11. Peak early currents from Figs. 8 and 9 plotted against surface potential. Note that the total current is less than the surface current at any particular voltage because the tubular capacity current is an outward current during depolarization. Estimates of V'_{Na} from the total current are in error. V'_{Na} in these calculations was set at + 50 mV.

DISCUSSION

The object of this paper has been the description of the action potential of a striated muscle fibre in terms of the ionic and capacity currents in the surface and transverse tubular membranes. In a number of respects the present model is an improvement on the simpler reconstruction of Adrian *et al.* (1970). It treats the tubular capacity as if it is distributed which it must be if the luminal conductance of the tubular lumen is less than infinite. It predicts a conduction velocity along the fibre which is similar to the experimental value. It predicts a humped after potential in some but not in all fibres, depending on the fibre diameter and other parameters.

The increased conduction velocity in the present model results from a number of relatively small adjustments in numerical values, which could equally well have been made on the simple model. For instance $\bar{g}_{Na}$ has been increased by 25 % and $\bar{\alpha}_m$ by about 10 % (see Table 1). But it is clear from Table 2 that within the range of tubular properties considered in this paper, an adequate longitudinal velocity depends on the presence of a resistance separating the extracellular fluid from the fluid in the tubular

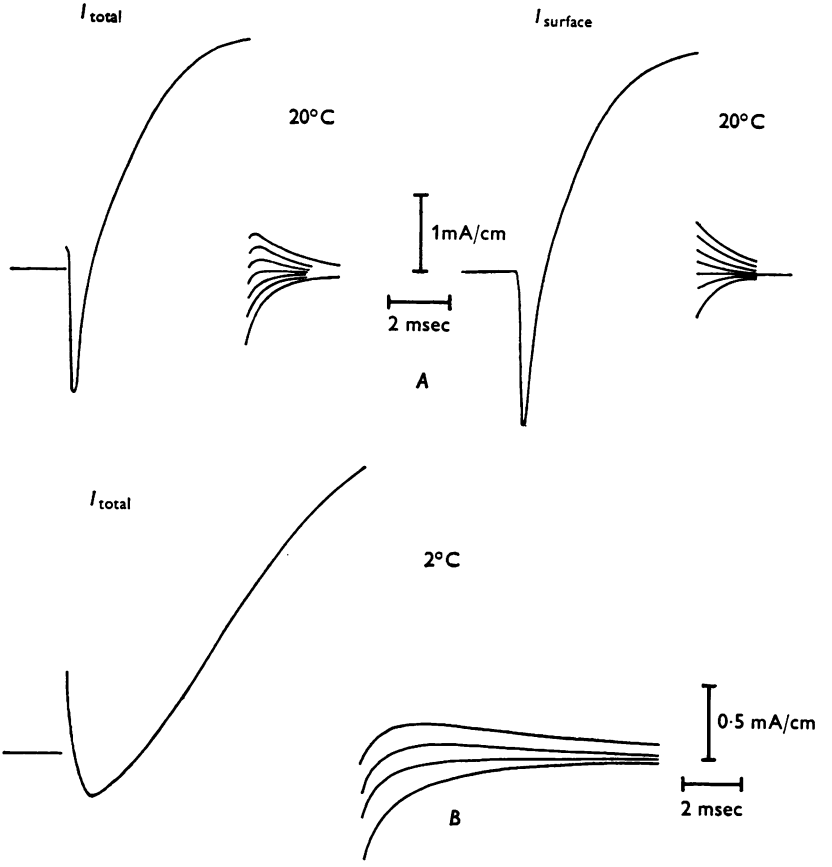

Fig. 12. Potassium tail currents. *A*: surface potential depolarized to 0 mV and returned to −100 mV, −90 mV, −85 mV, −80 mV, −75 mV, −70 mV, −65 mV. $V'_K = -85$ mV. Calculated surface currents at 20° C (right) show a clear zero change potential at −85 mV. Total currents (at left) suggest that the best estimate of the zero current potential would have been −80 mV. *B*: 2° C; surface potential depolarized to 30 mV and tail currents calculated at −90 mV, −85 mV, −80 mV and −75 mV. At this temperature the zero current potential would be estimated at or near the actual value (−85 mV). Fibre radius 60 μm. Numerical values as in Figs. 8 and 9.

lumen. It is this resistance that has been called the access resistance. It is possible that other combinations of lumen conductivity (G_L) and access resistance (R_s) could be chosen and that these would give reasonable reconstructions of the action potential. The results of Falk & Fatt (1964) and of Schneider (1970) require a greater radial resistance than would be present in our model without access resistance (Figs. 2*C*, 3, 4). It is not clear from these studies whether this radial resistance should be wholly lumped, wholly distributed, or something in between. Our model with access resistance (Figs. 2*A*, 6) making up the greater part of the radial resistance, is closer to a lumped model than to a totally distributed model. But our calculations suggest that decreasing the lumen conductivity (G_L) below the value used here (10 mmho cm^{-1}) substantially increases the radial conduction time. It has already been pointed out that in the reconstruction of Figs. 2*A* and 6 the predicted radial conduction speed is about half that deduced from the results of Gonzalez-Serratos (1971). This comparison depends on an assumption that the delay between the peak potential change and the contraction is the same at each radial position in the fibre. We do not know enough about the effect of wave form on the threshold to be certain that this is so (Adrian *et al.* 1969).

Fig. 2*A* raises the question, is the potential change across the tubular wall at the edge of the fibre, just inside the access resistance, adequate to cause contraction? Information about the potential change across the tubular wall which does or does not cause contraction is necessarily indirect. By an experiment at room temperature which imposed a potential change with the shape of an action potential on a muscle fibre poisoned with tetrodotoxin (Adrian, Costantin & Peachey, 1969), showed that the surface potential needs to reach approximately 0 mV if it is to cause the superficial myofibrils to contract. The interpretation of this observation in terms of a mechanically effective potential change across the tubular wall depends upon the model considered. Suppose that mechanical activation is only produced by tubular potential change, then if the access resistance is as large as 150 Ω cm^2 a brief surface depolarization to 0 mV will be attenuated by the access resistance, and one would have to suppose that the transient depolarization to about -45 mV is a threshold signal for contraction. On the other hand, if the surface potential change can activate the superficial myofibrils, then one would conclude that a brief depolarization to 0 mV is the effective signal in the surface and so probably in the tubules. There is no direct evidence for mechanical activation by surface potential change and the usual interpretation of experiments involving glycerol 'detubulation' (Eisenberg & Gage, 1967) argues against it. Nevertheless, it remains a possibility that 'detubulating' procedures do something more than break the tubules at their mouths; for instance they may also interfere with the triads

and with contacts between surface and sarcoplasmic membranes which would presumably be necessary for an activation by the surface potential change (Zachar, Zacharova & Adrian, 1972; Peachey & Adrian, 1973). It is possible that the access resistance is not at the tubular mouths, but is just inside the most superficial layer of myofibrils. There is no morphological evidence to suggest this position, but it would make it unnecessary to postulate activation by the surface membrane, and it might go some way to explain the circumferential propagation of activation observed by Sugi & Ochi (1967).

The model that we are proposing for the action potential in frog striated muscle has modified the explanation of the negative after-potential proposed by Persson (1963) and by Adrian *et al.* (1970). The latter estimated the zero-current potential of the delayed rectifier current ($V_K' = -70$ mV) and noted that it was similar to the membrane potential during the after potential (-60 to -75 mV; Persson, 1963). They suggested that the potassium to sodium permeability ratio of the delayed rectifier is about 30 which would account for the fact that the zero-current potential was positive to the resting potential. For as long as the delayed rectifier is open after an action potential the membrane potential would be held near to V_K'; in so far as there were currents recharging the capacity of the tubules, the potential would be positive to V_K'.

In the present calculations, the mechanism of the after potential is not essentially changed, but the relative importance of the tubular capacity currents has been altered. From the calculation in Fig. 12 it is clear that the measured tail current after a depolarization will be made up of tubular currents, mainly capacitative, and delayed rectifier current in the fibre surface. These two currents may either add or subtract. At 20° C these two components of current can decay at more or less the same rate and the measured zero-current potential (V_K' in Adrian *et al.* 1970) will not be the true zero-current potential (V_K' in the present paper), but will be positive to it. In the present calculation V_K' has been set somewhat arbitrarily at -85 mV. The calculated zero-current potential which would have been measured at 20° C is between -70 and -75 mV (total current, Fig. 12). The calculated potential at the beginning of the after potential is about -60 mV, which agrees well with the measured mean in Table 3 of -64 mV. We have not tested whether the present model will show a correlation between the resting potential and the potential during the after potential (Persson, 1963), but there seems no obvious mechanism by which it could do so. As can be seen from Fig. 2*A*, a substantial current is flowing into the tubular system through the access resistance during the period of the after potential, and it is largely this current which keeps the surface potential positive to V_K'. The after potential and the experimentally measured zero-

current potential are both positive to V'_K for the same reason: the capacity currents of the tubular system flow for several milliseconds after a voltage clamp step at the fibre surface: tubular currents are flowing for several milliseconds after the surface of the fibre has repolarized in the action potential.

A question that arises in connexion with sodium currents in the tubular membrane is possible depletion of tubular sodium ions. This might occur during an action potential or during a train of action potentials in a time too brief for significant replenishment of sodium ions by diffusion from the external medium. The present model does not incorporate any tubular concentration changes that might result from activity, but one can estimate the approximate concentration change by comparing the charge transferred across the tubular capacity and the quantity of sodium ions associated with unit area of membrane. If the initial tubular sodium concentration is $[Na]_t$, the fraction of this which would change the potential across the tubular wall by ΔV is given by $(C_W \Delta V)/(F[Na]_t \zeta)$. For $[Na]_t = 120$ mM and $\Delta V = 125$ mV, this fraction is about equal to 10^{-2}. This fraction suggests that the tubular sodium concentration might change by as much as 1 mM as the result of a single action potential. Various factors could alter the precise figure: over-lapping of the sodium and potassium conductance changes could increase it; radial current flow and the radial diffusion of sodium will both decrease the concentration change. For the fibre with a radius of 50 μm and the standard conductance parameters (Fig. 2), the integrated sodium current in the axial disk of the model (section 1 of the radial cable) would, for a complete action potential, result in a sodium concentration change there of $-0{\cdot}5$ mM. The calculated change in the potassium concentration at the axis of the fibre is $+0{\cdot}28$ mM. Significant changes in tubular ionic concentrations are therefore a consequence of the model for the action potential proposed in this paper. Tubular sodium depletion during a tetanus has already been suggested on experimental grounds (Bezanilla, Caputo, Gonzalez-Serratos, & Venosa, 1972).

We are grateful to Dr W. K. Chandler for advice and help; also to Mr A. Stracciolini for help with the plotting programs.

REFERENCES

ADRIAN, R. H. (1956). The effect of internal and external potassium concentration on the membrane potential of frog muscle. *J. Physiol.* **133**, 631–658.

ADRIAN, R. H., CHANDLER, W. K. & HODGKIN, A. L. (1969). The kinetics of mechanical activation in frog muscle. *J. Physiol.* **204**, 207–230.

ADRIAN, R. H., CHANDLER, W. K. & HODGKIN, A. L. (1970). Voltage clamp experiments in striated muscle fibres. *J. Physiol.* **208**, 607–644.

ADRIAN, R. H., COSTANTIN, L. L. & PEACHEY, L. D. (1969). Radial spread of contraction in frog muscle fibres. *J. Physiol.* **204**, 231–257.

BEZANILLA, F., CAPUTO, CARLO, GONZALEZ-SERRATOS, H. & VENOSA, R. A. (1972). Sodium dependence of the inward spread of activation in isolated twitch muscle fibres in the frog. *J. Physiol.* **223**, 507–523.

COSTANTIN, L. L. (1970). The role of sodium current in the radial spread of contraction in frog muscle fibres. *J. gen. Physiol.* **55**, 703–715.

EISENBERG, R. S. & GAGE, P. (1967). Frog skeletal muscle fibres. Changes in electrical properties after disruption of transverse tubular system. *Science, N.Y.* **158**, 1700–1701.

FALK, G. & FATT, P. (1964). Linear electrical properties of striated muscle fibres observed with intracellular electrodes. *Proc. R. Soc.* B **160**, 69–123.

FITZHUGH, R. (1966). Theoretical effect of temperature on threshold in the Hodgkin–Huxley nerve model. *J. gen. Physiol.* **49**, 989–1005.

FITZHUGH, R. & ANTOSIEWICZ, A. (1959). Automatic computation of nerve excitation – detailed corrections and additions. *J. Soc. indust. appl. Math.* **7**, 447–458.

GONZALEZ-SERRATOS, H. (1971). Inward spread of activation in vertebrate muscle fibres. *J. Physiol.* **212**, 777–799.

HODGKIN, A. L. & HUXLEY, A. F. (1952). A quantitative description of membrane current and its application to conduction and excitation in nerve. *J. Physiol.* **117**, 500–544.

HODGKIN, A. L. & NAKAJIMA, S. (1972*a*). The effect of diameter on the electrical constants of frog skeletal muscle fibres. *J. Physiol.* **221**, 105–120.

HODGKIN, A. L. & NAKAJIMA, S. (1972*b*). Analysis of the membrane capacity in frog muscle. *J. Physiol.* **221**, 121–136.

HUXLEY, A. F. & TAYLOR, R. E. (1958). Local activation of striated muscle fibres. *J. Physiol.* **144**, 426–441.

ILDEFONSE, M. & ROY, G. (1972). Kinetic properties of the sodium current in striated muscle fibres on the basis of the Hodgkin–Huxley theory. *J. Physiol.* **227**, 419–431.

PEACHEY, L. D. (1965). The sarcoplasmic reticulum and transverse tubules of the frog's sartorius. *J. Cell Biol.* **25**, 209–231.

PEACHEY, L. D. (1973). Electrical events in the *T*-system of frog striated muscle. *Cold Spring Harb. Symp. quant. Biol.* **37**, 479–488.

PEACHEY, L. D. & ADRIAN, R. H. (1973). Electrical properties of the transverse tubular system. In *Structure and Function of Muscle*, vol. 3, ed. BOURNE, G. New York: Academic Press.

PERSSON, A. (1963). The negative after-potential of frog skeletal muscle fibres. *Acta physiol. scand.* **58**, suppl. 205.

SCHNEIDER, M. F. (1970). Linear electrical properties of the transverse tubules and surface membrane of skeletal muscle fibres. *J. gen. Physiol.* **56**, 640–671.

SUGI, H. & OCHI, R. (1967). The mode of transverse spread of contraction initiated by local activation in single frog fibres. *J. gen. Physiol.* **50**, 2167-2176.

ZACHAR, J., ZACHAROVA, D. & ADRIAN, R. H. (1972). Observations on 'detubulated' muscle fibres. *Nature, New Biol.* **239**, 153–155.